Indian Journal of Pure & Applied Physics
Vol. 54, October 2016, pp. 641-650

Engineering optical properties of double quantum well systems

Poonam Silotia[a]*, Rajesh Giri[b] & Vinod Prasad[c]

[a]Department of Physics and Astrophysics, University of Delhi, Delhi 110 007, India

[b]Department of Physics, Rajdhani College, University of Delhi, Delhi 110 015, India

[c]Department of Physics, Swami Shraddhanand College, University of Delhi, Delhi 110 036, India

Received 29 April 2015; revised 14 July 2016; accepted 9 August 2016

Linear, nonlinear and total absorption coefficient and refractive index changes of double quantum well systems have been studied theoretically in the presence of external magnetic field applied along the growth direction. The analytical expressions for the linear and nonlinear optical properties have been obtained using density matrix method. The optical properties have been studied in detail for various quantum well shapes, e.g., rectangular, triangular and parabolic, and laser parameters. Shape effects play an important role in modifying the response of quantum heterostructures to external fields. The role of asymmetry parameter on quantum well optical properties has been emphasized.

Keywords: Asymmetry parameter, Quantum well, Absorption coefficient, Refractive index changes

1 Introduction

Optical phenomena based on intersubband transitions in semiconductor quantum heterostructures have gained considerable interest in recent years. Due to quantum-confinement effect, the nonlinear effects can be enhanced to a great extent in these low-dimensional quantum systems as compared to those in bulk materials. Both the linear and nonlinear processes have been widely investigated[1-6] in these structures due to their large values of dipole matrix elements. In the literature, several theoretical analyses on the absorption coefficients and changes in the refractive index associated with intersubband optical transitions in single-quantum well and multiple quantum wells are presented.

Double quantum well (DQW) systems have been studied in great detail for the last few decades due to various reasons. Immediately after first experimental realization of $GaAs/Ga_{1-x}Al_xAs$ quantum wells (QWs)[7,8], QWs and in particular, double quantum wells (DQWs), have been a subject of immense theoretical and experimental studies[9,10]. As DQWs show effect of tunneling coupling quite interestingly, the wave functions of the different wells overlap in the barrier region and show splitting of sub-band energy levels. Of course, this splitting depends on a number of factors such as ratio of well widths, doping concentration, and barrier width etc. In addition, the realization of such quantum systems led to the development of many new optoelectronic devices e.g. photodetectors[11], semiconducting diodes[12] etc.

Further, DQW systems have applications in emitting laser light in a wide range of wavelengths including 1.3-1.5 μm, which is very useful in optical communications. Terahertz detectors have also been fabricated[13,14]. Various devices have been fabricated by varying the potential profile of a DQW system and multiple quantum wells[15-18]. The electric field effects on the refractive index and optical absorption coefficient has been investigated by Kanet *et al*[19] in 1987. Chuang and Ahn[20] reported the variation of linear refractive index and absorption coefficients in a parabolic quantum well. Linear and nonlinear optical absorptions in semiconductor superlattice systems were also recently investigated[21].

Recently, there has been a new surge in the field of effect of shape of the system on optical properties. Different shapes of DQW systems were proposed and studied experimentally by Shim *et al*[22,23]. Choi *et al*[24] studied influence of QW shape on the light emission characterization and light emitting diodes and experimentally realized blue light emitting diode of InGaN/GaN. While triangular quantum wells have been studied for many practical purposes[25-28] with InGaN/GaN triangular shaped MQWs but asymmetric double quantum well (ADQW) systems with

*Corresponding author (E-mail: psilotia.du@gmail.com)

rectangular shapes exposed to laser fields are subject of major chunk of the studies devoted to quantum heterostructures.

In addition to rectangular and triangular shapes, other shapes of DQW which have received attention are some peculiar cases e.g. parabolic[29-31], graded[32], semi-parabolic and semi-inverse squared etc.[33,34] These results show that shapes of quantum wells play an important role in determining the properties of QW systems.

The static magnetic field applied along the growth direction affects the quantum states of the quantum well. The two fold degeneracy of the levels present in the symmetric DQW system gets lifted when the external magnetic field is applied. For ADQW, the degeneracy is already lifted because of the difference in widths of the wells. When external field is applied, there is a further increase in the energy difference between different levels leading to drastic change in the transition matrix elements. One can infer that ADQW structure holds greater applicability than symmetric double quantum well (SDQW)[35]. Recently, we have reported the effect of asymmetry on the optical properties of a rectangular QDW system in the presence of external electric field[36].

In this work, in addition to asymmetry, the applied static field greatly modifies the energy levels and the transition matrix elements between levels. Further, we study, optical absorption coefficients and refractive index changes of a coupled DQW system in the presence of external magnetic field. In particular, we focus on the effect of shape and asymmetry on the optical properties of DQW systems.

2 Theory

In this section, the eigen states and eigen energies in the ADQWs will be discussed and the formalism for the derivation of linear and nonlinear refractive index changes will be presented. For simplicity, an idealised ADQW heterostructure model is considered, where the band non-parabolicity and the variation of effective masses in different layers, are neglected.

By the effective mass approximation, the electron Hamiltonian in this ADQW is well described by:

$$H = -\frac{\hbar^2}{2m^*}\left(\frac{\partial^2}{\partial z^2}\right) + V(z) \quad \ldots (1)$$

where z represents the growth direction of the quantum well, $\hbar = h/2\pi$, h being the Planck's constant, m^* is the effective mass of the conduction band. Let the conduction band potential in the quantum well be V_0.

The Hamiltonian in the presence of external magnetic field B becomes:

$$H = -\frac{\hbar^2}{2m^*}\left(\frac{\partial^2}{\partial z^2}\right) + V(z) + \frac{e^2B^2z^2}{2m^*} \quad \ldots (2)$$

The time independent Schrodinger equation:

$$H\Psi_n(z) = E_n\Psi_n(z) \quad \ldots (3)$$

Where $\Psi_n(z)$ is the wave function and E_n is the corresponding eigen energy obtained by solving the time independent Schrodinger equation using finite difference method.

Let us consider the system be excited by the monochromatic electromagnetic field given by $\boldsymbol{E}(t) = \boldsymbol{E}\exp(i\omega t) + \boldsymbol{E}\exp(-i\omega t)$, which is incident with a polarization vector normal to the quantum wells. The evolution of the one electron density matrix ρ is given by the time-dependent Schrodinger equation:

$$\frac{\partial \rho_{ij}}{\partial t} = \frac{1}{i\hbar}[H_0 - qzE(t), \rho]_{ij} - \Gamma_{ij}(\rho - \rho^{(0)})_{ij} \quad \ldots (4)$$

where H_0 is the Hamiltonian of this system without the incident field $\boldsymbol{E}(t)$, q is the electronic charge, $\rho^{(0)}$ is the unperturbed density matrix, and Γ_{ij} is the relaxation rate.

Next, we calculate the absorption coefficients and the refractive index changes based on linear susceptibility $\chi^{(1)}$ and the third order susceptibility $\chi^{(3)}$, which are derived using the density matrix method[37].

Following the usual procedure to evaluate the optical properties, we calculate the polarization $\boldsymbol{P}(t)$ of the quantum system due to $\boldsymbol{E}(t)$ as:

$$P(t) \approx \varepsilon_0\chi^{(1)}(\omega)\vec{E}(i\omega t) + \varepsilon_0\chi^{(3)}(\omega)\vec{E}(i\omega t) \quad \ldots (5)$$

where ε_0 is the permittivity of vacuum and $\chi^{(n)}$ are the n^{th} order susceptibilities of the quantum well material.

The analytical expressions for the $\chi^{(1)}$ and $\chi^{(3)}$ are given as[38,39]:

$$\epsilon_0\chi^{(1)}(\omega) = \frac{N|\mu_{ji}|^2}{E_{ji} - \hbar\omega - i\hbar\tau_{ji}} \times \frac{(E_{ji} - \hbar\omega + i\hbar\tau_{ji})}{(E_{ji} - \hbar\omega + i\hbar\tau_{ji})} \quad \ldots (6)$$

and

$$\epsilon_0\chi^{(3)}(\omega) = \frac{N|\mu_{ji}|^2E^2}{(E_{ji} - \hbar\omega - i\hbar\tau_{ji})} \times \left[\frac{4|\mu_{ji}|^2}{(E_{ji} - \hbar\omega)^2 + (\hbar\tau_{ji})^2} - \frac{(\mu_{22} - \mu_{11})^2}{(E_{ji} - i\hbar\tau_{ji})(E_{ji} - \hbar\omega - i\hbar\tau_{ji})}\right] \quad \ldots (7)$$

It is well known that the susceptibility χ(ω) is related to the change in the refractive index as:

$$\frac{\Delta n(\omega)}{n_r} = Re\,\frac{\chi(\omega)}{2n_r^2} \quad \ldots (8)$$

where n_r is the refractive index. By using Eqs. 6 and 7 we get:

$$\frac{\Delta n^{(1)}(\omega)}{n_r} = \frac{1}{2n_r^2\epsilon_0}|\mu_{ji}|^2 N\left[\frac{E_{ji}-\hbar\omega}{(E_{ji}-\hbar\omega)^2+(\hbar\tau_{ij})^2}\right] \quad \ldots (9)$$

$$\frac{\Delta n^{(3)}(\omega)}{n_r} = \frac{-\mu c}{4n_r^3\epsilon_0}|\mu_{ji}|^2 \frac{NI}{\left[(E_{ji}-\hbar\omega)^2+(\hbar\tau_{ij})^2\right]^2}$$
$$\left[4(E_{ji}-\hbar\omega)|\mu ji|^2 - \frac{(\mu_{jj}-\mu_{ii})^2}{(E_{ji})^2+(\hbar\tau_{ij})^2}\right]$$
$$\times\left[(E_{ji}-\hbar\omega)\left[E_{ji}(E_{ji}-\hbar\omega)-(\hbar\tau_{ji})^2\right]-(\hbar\tau_{ji})^2(2E_{ji}-\hbar\omega)\right] \quad \ldots (10)$$

$$I = \left(\frac{\epsilon_r}{\mu}\right)^{1/2}|E(\omega)|^2 = \frac{2n_r}{\mu c}|E(\omega)|^2 = 2\epsilon_0 n_r c|E(\omega)|^2 \quad \ldots (9)$$

where c is the speed of light in free space.

In Eqs. 5-8, N is the carrier density in this system, μ is the permeability of the system, $E_{ji} = E_j - E_i$ is the energy difference of the two different electronic states of the system. μ_{ij} are the matrix elements defined as $\mu_{ij} = \langle\psi_j|ez|\psi_i\rangle$. I is the incident optical intensity. Γ is the phenomenological operator. Non-diagonal elements Γ_{ji} ($j \neq i$) called as the relaxation rate of the j^{th} to the i^{th} state. Γ_{ji} is related to the relaxation time as $(\Gamma_{ji})=1/\tau_{ji}\}$. τ_{ji} is taken to be 0.14 ps.

$$\frac{\Delta n_r(\omega)}{n_r} = \frac{\Delta n^{(1)}(\omega)}{n_r} + \frac{\Delta n^{(3)}(\omega)}{n_r} \quad \ldots (12)$$

Finally the total absorption coefficient α(ω,I) is given as:

$$\alpha(\omega, I) = \alpha^{(1)}(\omega) + \alpha^{(3)}(\omega, I) \quad \ldots (13)$$

with

$$\alpha^{(1)}(\omega) = \omega\left(\frac{\mu}{\epsilon_r}\right)^{1/2}\frac{|\mu_{ji}|^2 N\hbar\tau_{ij}}{(E_{ji}-\hbar\omega)^2+(\hbar\tau_{ij})^2} \quad \ldots (14)$$

$$\alpha^{(3)}(\omega) =$$
$$-\omega\left(\frac{\mu}{\epsilon_r}\right)^{1/2}\left(\frac{I}{2\epsilon_0 n_r c}\right)\frac{|\mu_{ji}|^2 N\hbar\tau_{ij}}{\left[(E_{ji}-\hbar\omega)^2+(\hbar\tau_{ij})^2\right]^2}\left[4|\mu_{ji}| - \frac{(\mu_{jj}-\mu_{ii})^2\left[3E_{ji}^2-4E_{ji}\hbar\omega+\hbar^2(\omega^2-\tau_{ij}^2)\right]}{(E_{ji})^2+(\hbar\tau_{ij})^2}\right] \quad \ldots (15)$$

3 Results and Discussion

In the numerical calculations of the absorption coefficients and the refractive index changes, we have taken the following parameters: effective mass, m^*=0.067 m_e, m_e is the free electron mass; dielectric constant of the material, ε = 12.4; number density of the electrons, $N = 10^{22}$ m^{-3}; relaxation time, τ_{ij}=1.0/0.14 ps^{-1} and refractive index of the material, n_r=3.2. In our results, we have taken Al concentration x=0.03 and potential, V_0 = 228 meV. The parameters chosen are suitable for GaAs/$Ga_{1-x}Al_xAs$ quantum well.

For the sake of understanding, in Fig. 1, we have shown the double quantum well shapes taken in the study. Also shown are $|\psi_n(z)|^2$ for the lowest four eigenstates of the system. Figures 1(a), 1(b) and 1(c)

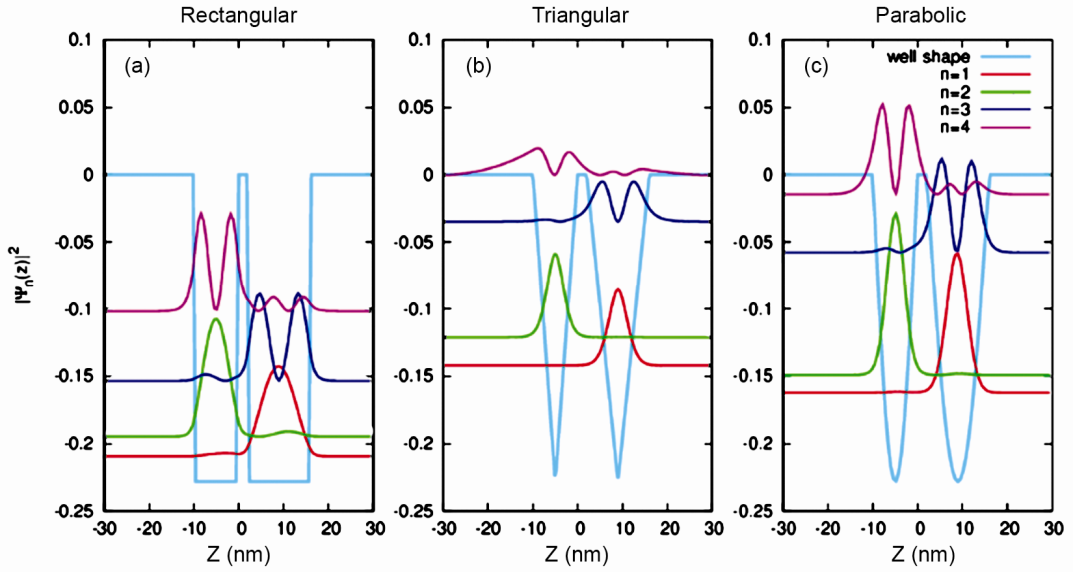

Fig. 1 – Structure of asymmetric double quantum well system of different shapes (a) rectangular, (b) triangular and (c) parabolic with asymmetry parameter 1.4, along with $|\psi_n(z)|^2$ for the lowest four eigen states of the system. Left well width=10 nm and barrier width= 2 nm

show rectangular, triangular and parabolic DQWs, respectively. In all three cases, the left well width is 10 nm and the barrier width is 2 nm. Whereas the right well width is 14 nm, thus defining the asymmetry parameter (A_p = Right well width/Left well width=1.4).

In Fig. 2(a), we present the variation of energy difference ($|E_2$-$E_1|$), between the ground and first excited state, with the asymmetry parameter, for all the three well shapes, in the absence as well as presence (B = 5T) of the magnetic field. The energy difference is minimum when A_p = 1.0 (symmetric well) and increases when A_p is varied on both sides of A_p = 1.0. Further, it is also shown that when A_p>1.0, the magnetic field influences the energy difference

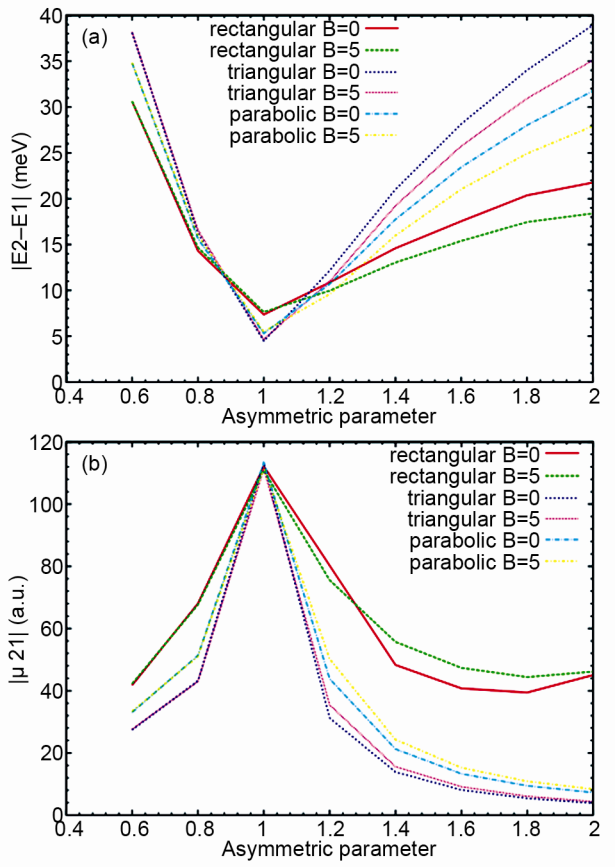

Fig. 2 – (a) Variation of energy difference of the states with the asymmetry parameter in the DQW of different rectangular, triangular and parabolic shapes. The different set of energy states is for the transition (2→ 1), i.e., E_2 - E_1 at magnetic field B=0 T and 5 T. Left well width=10 nm and barrier width= 2 nm. (b) Variation of dipole matrix elements with the asymmetry parameter in the DQW of different rectangular, triangular and parabolic shapes. The energy transition is taken to be from is for the transition (2→ 1), i.e., μ_{21} at magnetic field B=0 T and 5 T. Left well width=10 nm and barrier width= 2 nm

significantly compared to the case when A_p<1.0. Hence, not only the shape but also asymmetry parameter becomes a tool to influence $\Delta E_{21} = |E_2$-$E_1|$. Figure 2(b) shows the transition matrix elements $|\mu_{21}|$, with the asymmetry parameter. We have shown two cases of magnetic field: B = 0 and B = 5T. In all the three cases of well shape, they have same value when A_p = 1.0. The value of transition matrix element decreases when A_p is varied on either side from A_p =1.0. We observed almost similar behaviour for all transition matrix elements.

Figure 3 shows the variation of linear absorption coefficient, $\alpha^{(1)}$ with laser frequency $\hbar\omega$ (meV) for the transition 2 →1. The QDW shape in this case is rectangular. The left well width is 10 nm, barrier width is 2 nm and the right well width is varied from 8 nm to 18 nm in steps of 2 nm as depicted by the asymmetry parameters on the top of the panels from (a)-(f). The variation of $\alpha^{(1)}$ in each case has been studied for various magnetic fields, B = 0, 2, 5, 8 and 10 T. The value of linear absorption coefficient, $\alpha^{(1)}$, is maximum for asymmetry parameter A_p = 1.0 corresponding to the symmetric double quantum well. The value of $\alpha^{(1)}$ decreases for A_p above and below 1.0 as is clear from the figure. Further, the value of $\alpha^{(1)}$ keeps decreasing with increasing value of A_p for a given value of magnetic field, and the peak value of $\alpha^{(1)}$ for a given magnetic field shifts to higher value of laser frequency when the asymmetry parameter increased, as it clear for the panels (c)-(f) in the figure. For lower values of A_p, the variation of $\alpha^{(1)}$ with the magnetic field is small, which becomes significant for DQW with higher values of asymmetry parameter. For a given values of A_p, the value of $\alpha^{(1)}$ keeps on increasing with increase in the magnetic field but the position of the peak value of $\alpha^{(1)}$ shifts to lower values of laser frequency, i.e., there is red shift.

Figures 4 and 5 show same variation for triangular and parabolic wells, respectively. The variation of $\alpha^{(1)}$ keeps decreasing with increasing value of A_p for a given value of magnetic field, i.e., $\alpha^{(1)}$ show the same trend as for the rectangular DQW, the only difference being in the values of $\alpha^{(1)}$. While the value of $\alpha^{(1)}$ for A_p = 1.2 and B = 10 T is ~ 8.97×10^5 m^{-1} for rectangular DQW, it is ~ 2.51×10^5 m^{-1} for triangular DQW and ~ 4.52×10^5 m^{-1} for parabolic DQW. Further, the variation of the value of $\alpha^{(1)}$ and the position of its peak value shows the same trend for triangular and parabolic DQW as for the rectangular DQW. This can be explained on the basis of the energy

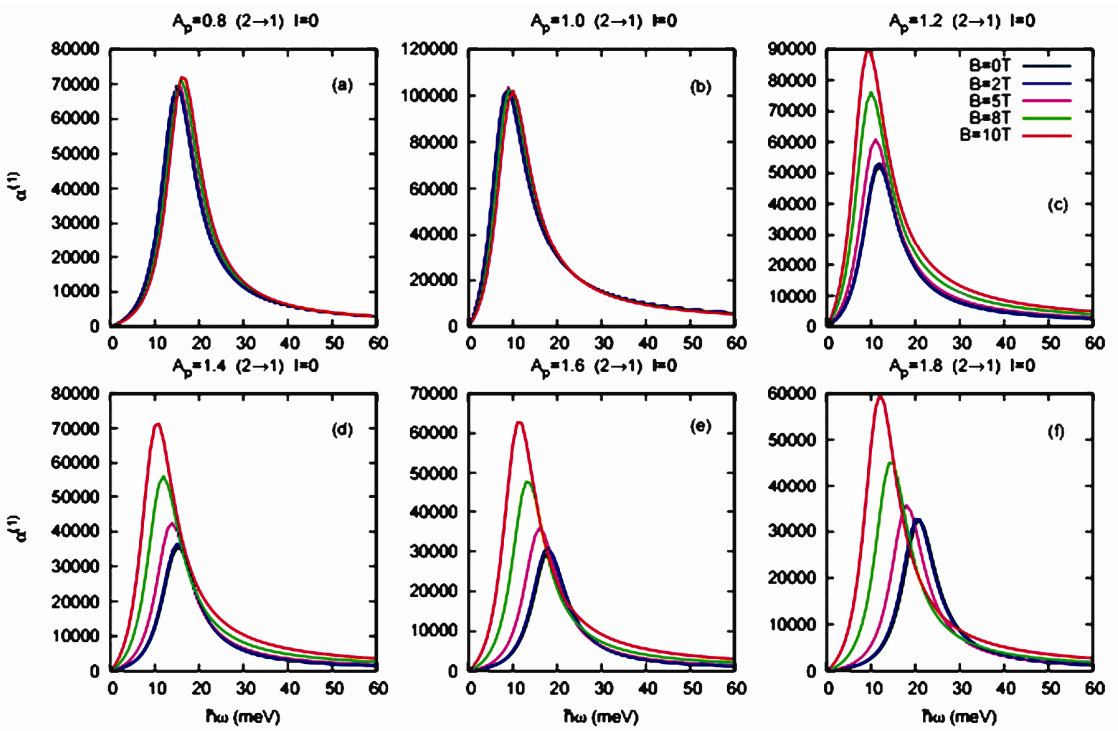

Fig. 3 – Variation of linear absorption coefficient, $\alpha^{(1)}$, in the rectangular DQW with laser frequency $\hbar\omega$ (meV) for the laser intensity, I=0 W/m^2 for magnetic fields = 0, 2, 5, 8 and 10 T. Left well width = 10 nm, barrier width = 2 nm. The asymmetry parameters for panels (a), (b), (c), (d), (e) and (f) are 0.8, 1.2, 1.4, 1.6 and 1.8, respectively. The energy transition is taken to be for the transition (2→ 1)

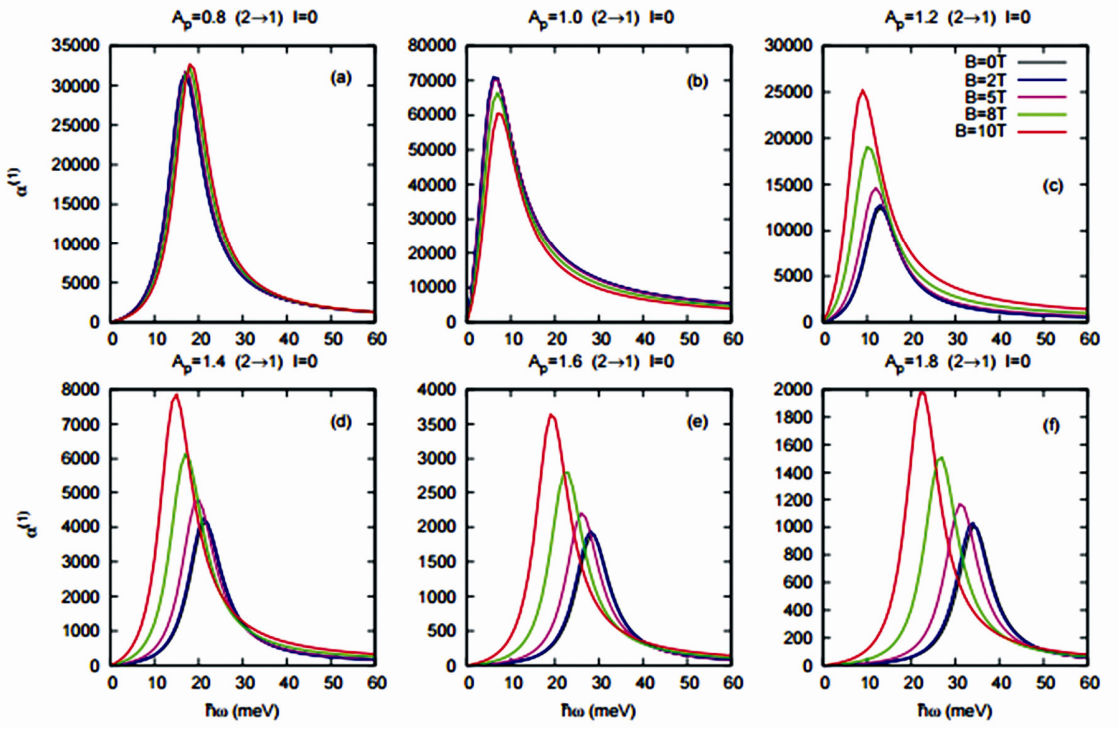

Fig. 4 – Variation of linear absorption coefficient $\alpha^{(1)}$, in the triangular DQW with laser frequency $\hbar\omega$ (meV) for the laser intensity, I=0 W/m^2 for magnetic fields = 0, 2, 5, 8 and 10 T. Left well width = 10 nm, barrier width = 2 nm. The asymmetry parameters for panels (a), (b), (c), (d), (e) and (f) are 0.8, 1.2, 1.4, 1.6 and 1.8, respectively. The energy transition is taken to be for the transition (2→ 1)

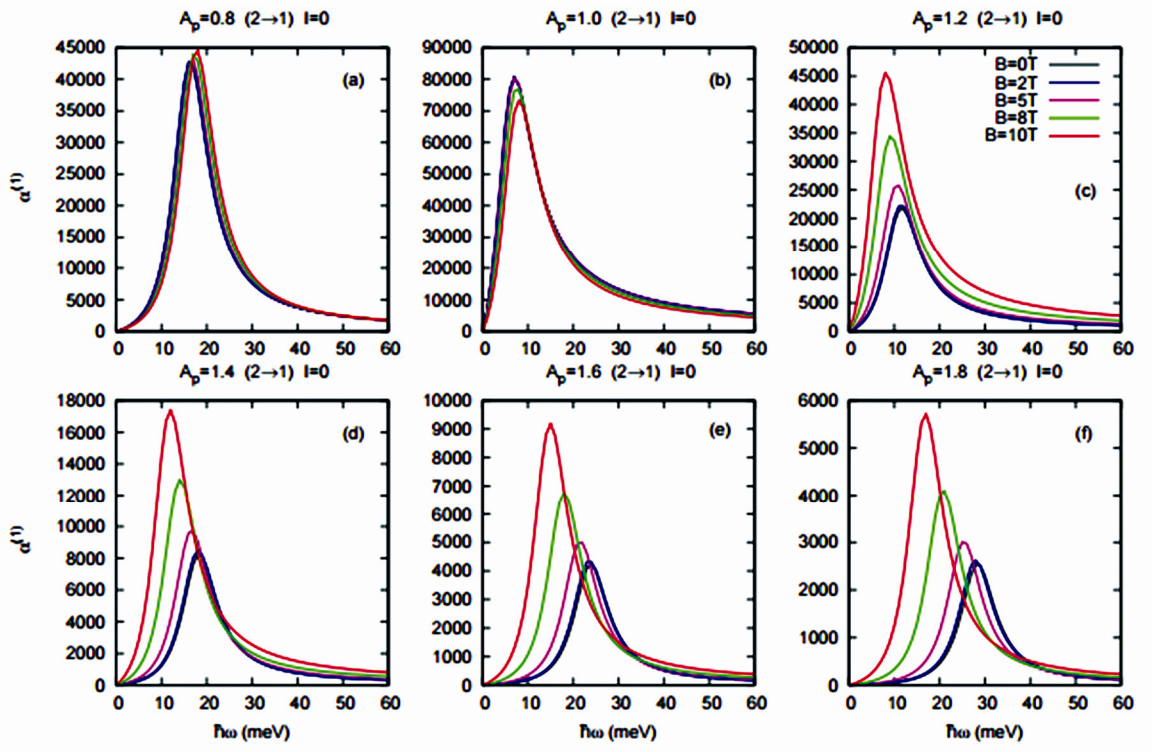

Fig. 5 – Variation of linear absorption coefficient, $\alpha^{(1)}$, in the parabolic DQW with laser frequency ħω (meV) for the laser intensity, I=0 W/m^2 for magnetic fields = 0, 2, 5, 8 and 10 T. Left well width = 10 nm, barrier width = 2 nm. The asymmetry parameters for panels (a), (b), (c), (d), (e) and (f) are 0.8, 1.2, 1.4, 1.6 and 1.8, respectively. The energy transition is taken to be for the transition (2→ 1)

difference and the transition matrix elements compared for all the three cases in Figs 2(a) and 2(b), respectively.

In Fig. 6, the variation of linear $\alpha^{(1)}$, nonlinear $\alpha^{(3)}$, and total α, absorption coefficient in the rectangular DQW with laser frequency ħω (meV) has been presented for different laser intensities for magnetic fields = 5T. The intensities I = 0, 0.2, 0.5, 0.8 and 1.0 correspond to I×10^{10} W/m^2. Left well width = 10 nm, barrier width = 2 nm. The asymmetry parameters for panels (a), (b), (c), (d), (e) and (f) are 0.8, 1.2, 1.4, 1.6 and 1.8, respectively. The energy transition is taken to be for the transition (2 → 1). The value of total absorption coefficient α is maximum for asymmetry parameter A_p = 1.0. The value of $\alpha^{(3)}$ keeps on increasing with increase in the laser intensity for the given value of A_p leading to lower value of α. For a given value of laser intensity the value of $\alpha^{(3)}$ keeps decreasing with increasing value of A_p leading to more linear effect.

Figures 7 and 8 show same variation for triangular and parabolic wells, respectively. For both triangular and parabolic DQW, the trend is same as that in the rectangular DQW. For A_p = 1.8, laser intensity I = 1.0×10^{10} W/m^2 and B = 5T, while the absolute value of nonlinear absorption coefficient $\alpha^{(3)}$ is more as compared to $\alpha^{(1)}$ leading to a negative value of α for rectangular DQW, the values of $\alpha^{(3)}$ as compared to $\alpha^{(1)}$ are less in the case of triangular and parabolic DQWs leading to positive values of α. These $\alpha^{(1)}$, $\alpha^{(3)}$ and α values are 3.56×10^5 m^{-1}, -2.72×10^6 m^{-1} and -2.37×10^6 m^{-1} for rectangular; 1.16×104 m^{-1}, -1.70×10^3 m^{-1} and 9.96×10^3 m^{-1} for triangular; and 3.09×10^4 m^{-1}, -1.40×10^4 m^{-1} and -1.60×10^4 m^{-1} for parabolic DQW, respectively. These values have their peak positions at laser frequency 18, 31 and 25 meV for rectangular, triangular and parabolic DQW, respectively, as is evident from the panel (f) of Figs 6, 7 and 8.

Figure 9 shows the variation of linear, $\Delta n_r^{(1)}/n_r$, non-linear, $\Delta n_r^{(3)}/n_r$ and total, $\Delta n_r/n_r$, refractive index changes in rectangular DQW for different asymmetry parameter, with laser frequency ħω (meV) for different laser intensities. The intensities I = 0, 0.2, 0.5, 0.8 and 1.0 correspond to I×10^{10} W/m^2. Left well width=10 nm, barrier width=2 nm. Asymmetry parameters taken in the figure are 0.8 in (a) and (d); 1.0 in (b) and (e); 1.2 in (c) and (f). The energy

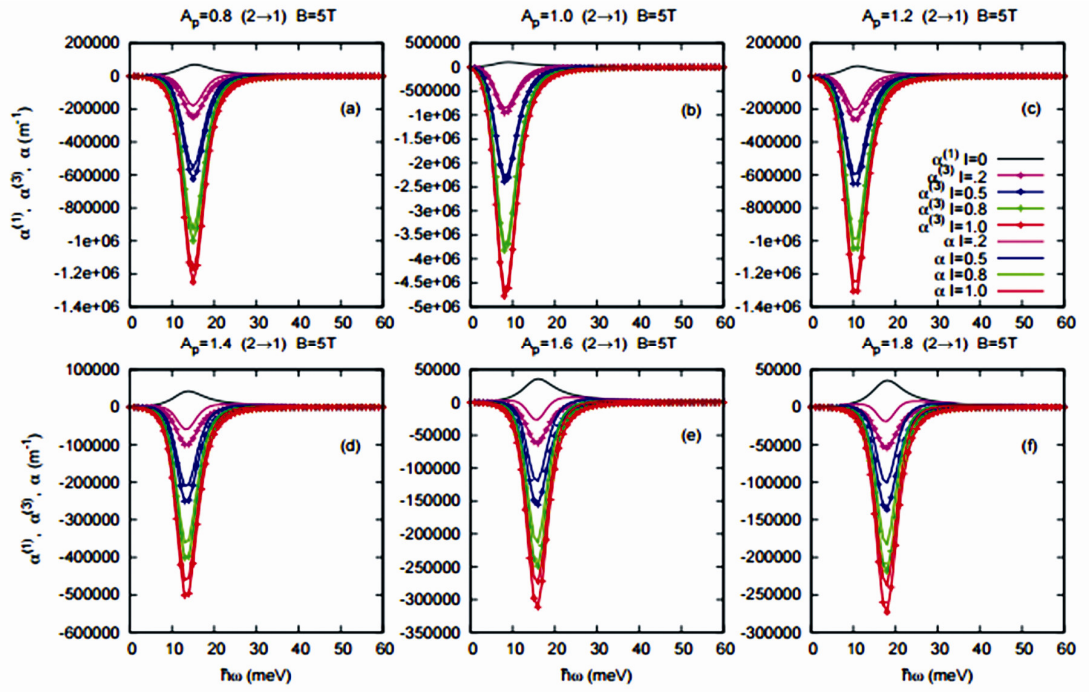

Fig. 6 – Variation of linear, $\alpha^{(1)}$, nonlinear, $\alpha^{(3)}$, and total, α, absorption coefficient in the rectangular DQW with laser frequency $\hbar\omega$ (meV) for different laser intensities for magnetic fields = 5 T. The intensities I=0, 0.2, 0.5, 0.8 and 1.0 correspond to $I\times10^{10}$ W/m^2. Left well width = 10 nm, barrier width = 2 nm. The asymmetry parameters for panels (a), (b), (c), (d), (e) and (f) are 0.8, 1.2, 1.4, 1.6 and 1.8, respectively. The energy transition is taken to be for the transition (2→ 1)

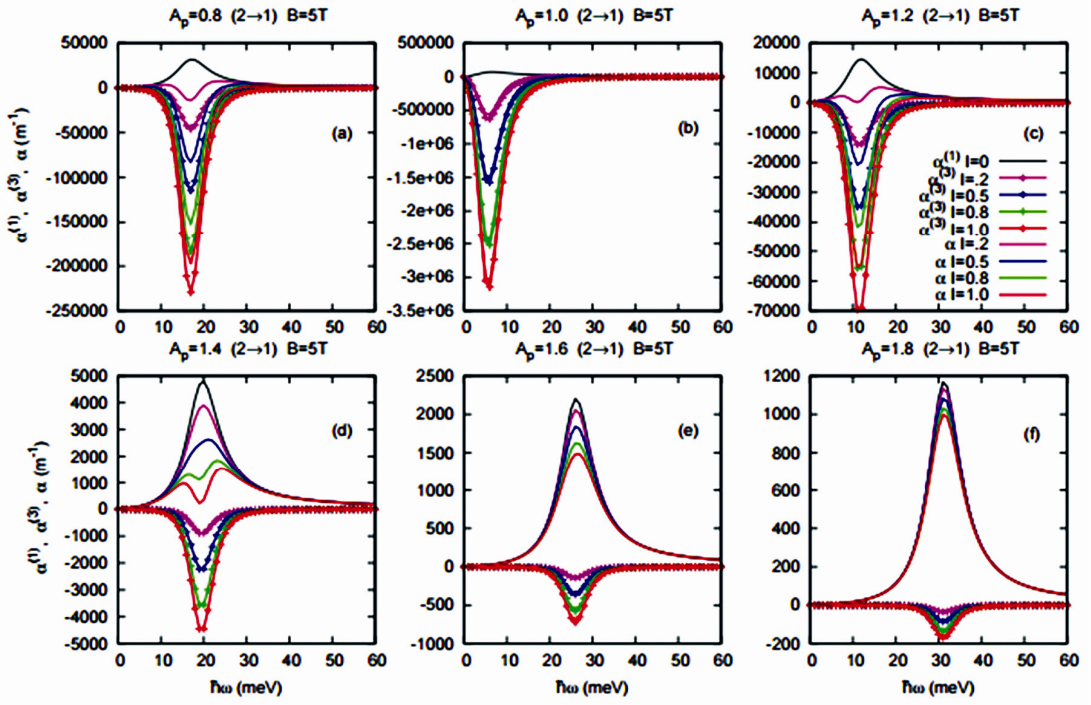

Fig. 7 – Variation of linear, $\alpha^{(1)}$, nonlinear, $\alpha^{(3)}$, and total, α, absorption coefficient in the triangular DQW with laser frequency $\hbar\omega$ (meV) for different laser intensities for magnetic fields = 5 T. The intensities I=0, 0.2, 0.5, 0.8 and 1.0 correspond to $I\times10^{10}$ W/m^2. Left well width = 10 nm, barrier width = 2 nm. The asymmetry parameters for panels (a), (b), (c), (d), (e) and (f) are 0.8, 1.2, 1.4, 1.6 and 1.8, respectively. The energy transition is taken to be for the transition (2→ 1)

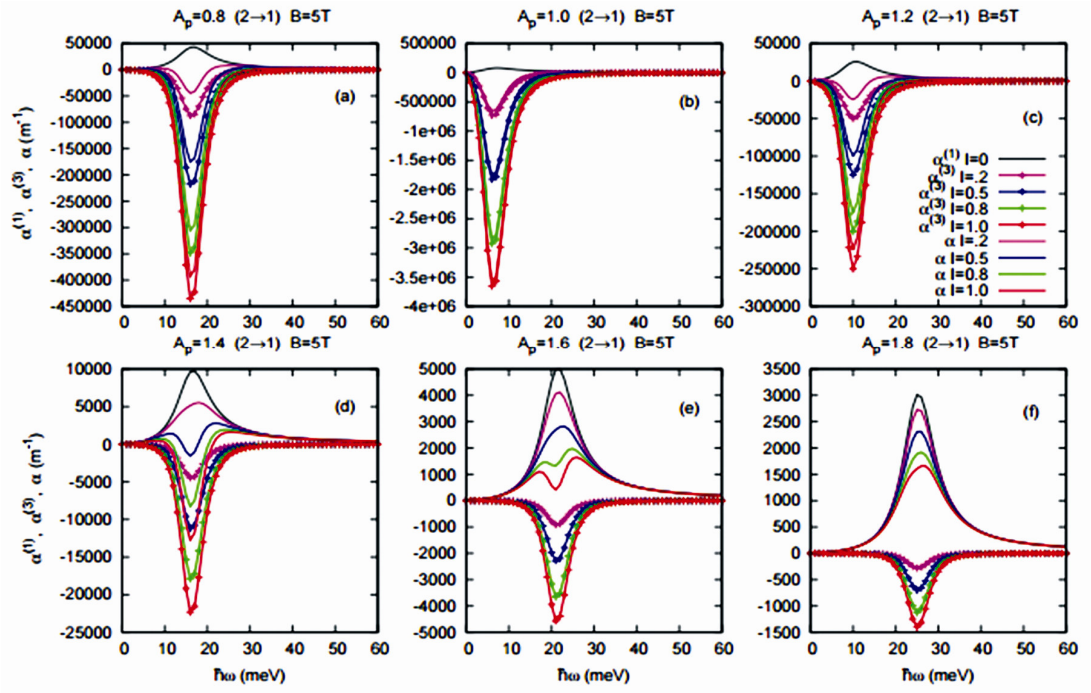

Fig. 8 – Variation of linear, $\alpha^{(1)}$, nonlinear, $\alpha^{(3)}$, and total, α, absorption coefficient in the parabolic DQW with laser frequency $\hbar\omega$ (meV) for different laser intensities for magnetic fields = 5 T. The intensities I=0, 0.2, 0.5, 0.8 and 1.0 correspond to $I\times10^{10}$ W/m^2. Left well width = 10 nm, barrier width = 2 nm. The asymmetry parameters for panels (a), (b), (c), (d), (e) and (f) are 0.8, 1.2, 1.4, 1.6 and 1.8, respectively. The energy transition is taken to be for the transition (2→ 1)

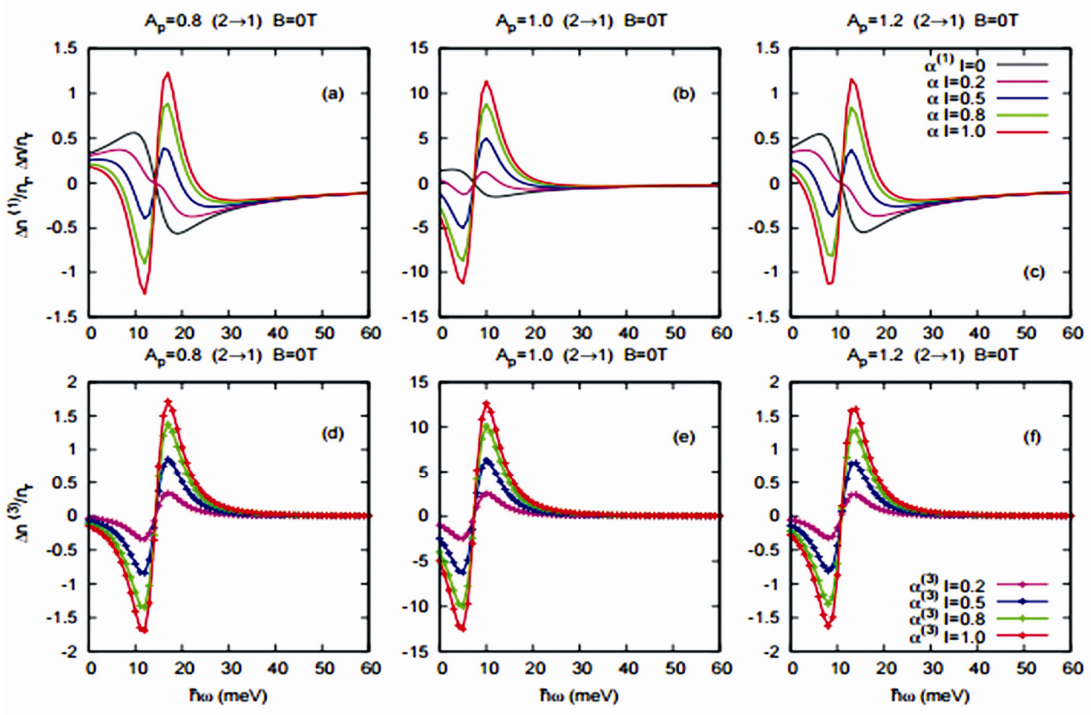

Fig. 9 – Variation of linear, $\Delta n_r^{(1)}/n_r$, non-linear, $\Delta n_r^{(3)}/n_r$ and total, $\Delta n_r/n_r$, refractive index changes in rectangular DQW for different asymmetry parameter, with laser frequency $\hbar\omega$ (meV) for different laser intensities. The intensities I=0, 0.2, 0.5, 0.8 and 1.0 correspond to $I\times10^{10}$ W/m^2. Left well width=10 nm, barrier width=2 nm. Asymmetry parameter 0.8 in (a) and (d); 1.0 in (b) and (e); 1.2 in (c) and (f). The energy transition is taken to be for the transition (2→ 1) and the magnetic field B is taken to be 0 T

transition is taken to be for the transition (2→ 1) and the magnetic field B is taken to be 0 T. The value of $\Delta n_r^{(3)}/n_r$ is maximum for the symmetric DQW.

Figures 10 and 11 show same variation for triangular and parabolic wells, respectively. The value of $\Delta n_r^{(1)}/n_r$, $\Delta n_r^{(3)}/n_r$, and $\Delta n_r/n_r$ for A_p =1.0 and

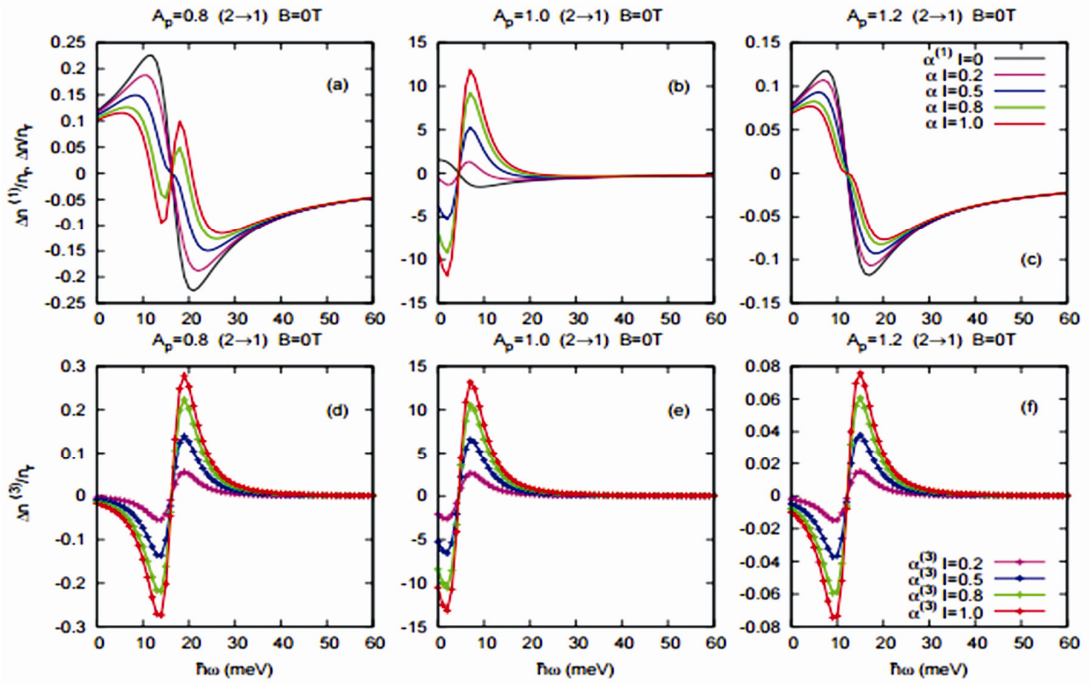

Fig. 10 – Variation of linear, $\Delta n_r^{(1)}/n_r$, non-linear, $\Delta n_r^{(3)}/n_r$ and total, $\Delta n_r/n_r$, refractive index changes in triangular DQW for different asymmetry parameter, with laser frequency $\hbar\omega$ (meV) for different laser intensities. The intensities I=0, 0.2, 0.5, 0.8 and 1.0 correspond to $I\times10^{10}$ W/m^2 Left well width=10 nm, barrier width=2 nm. Asymmetry parameter 0.8 in (a) and (d); 1.0 in (b) and (e); 1.2 in (c) and (f). The energy transition is taken to be for the transition (2→ 1) and the magnetic field B is taken to be 0 T

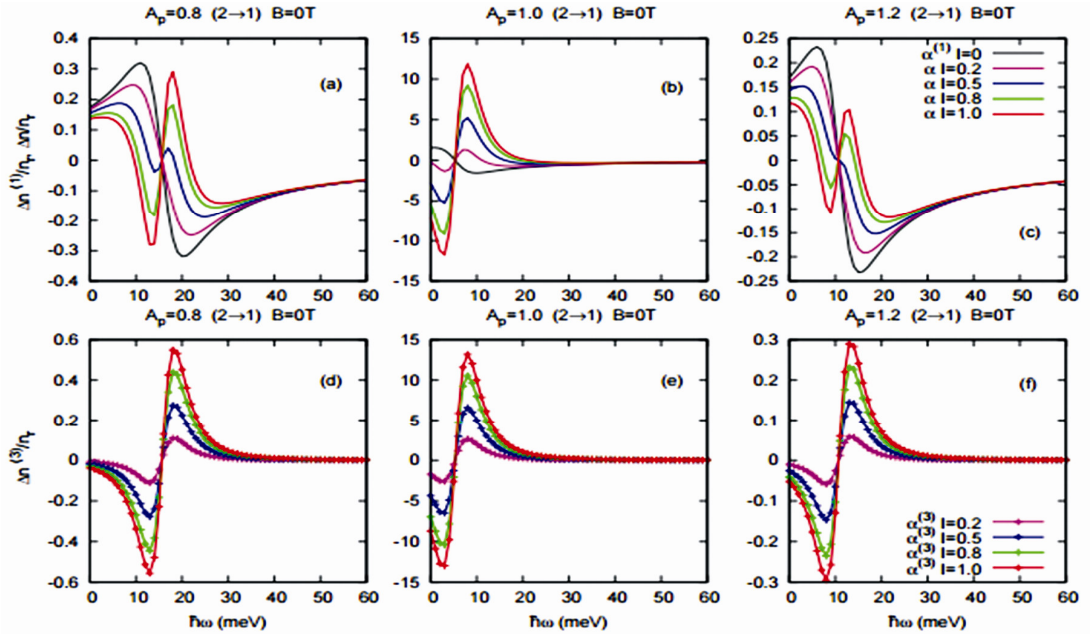

Fig. 11 – Variation of linear, $\Delta n_r^{(1)}/n_r$, non-linear, $\Delta n_r^{(3)}/n_r$ and total, $\Delta n_r/n_r$, refractive index changes in parabolic DQW for different asymmetry parameter, with laser frequency $\hbar\omega$ (meV) for different laser intensities. The intensities I=0, 0.2, 0.5, 0.8 and 1.0 correspond to $I\times10^{10}$ W/m^2. Left well width=10 nm, barrier width=2 nm. Asymmetry parameter 0.8 in (a) and (d); 1.0 in (b) and (e); 1.2 in (c) and (f). The energy transition is taken to be for the transition (2→ 1) and the magnetic field B is taken to be 0 T

I =1.0×10^{10} W/m^2 for various shapes of symmetric DQW are -1.48, 11.69 and 10.21 at $\hbar\omega$ = 11 meV for rectangular; -1.31, 13.17 and 11.86 at laser frequency $\hbar\omega$ = 7 meV for triangular; and -1.35, 13.17 and 11.82 at $\hbar\omega$ = 8 meV for parabolic. The corresponding values for the asymmetric DQW with A_p =1.2 and I =1.0×10^{10} W/m^2 are -0.18, 0.28 and 0.10 at $\hbar\omega$ = 13 meV for rectangular; -.10, .07 and -0.03 at $\hbar\omega$ = 15 meV for triangular; and -0.51, 1.59 and 1.08 at $\hbar\omega$ = 14 meV for parabolic.

4 Conclusions

The optical properties namely linear and nonlinear absorption coefficients and changes in the refractive index of DQW system having different well shapes have been studied theoretically in detail for various quantum well and laser parameters in the presence of external magnetic field applied along the growth direction. The role of asymmetry parameter, in particular, has been emphasized. It is shown that the magnetic field along with asymmetry parameter may prove vital for engineering optical properties of coupled quantum well systems. Further, it is shown that asymmetry parameter A_p>1 influences the absorption coefficients and refractive index changes quite strongly as compared to the case when A_p <1. There are shifts in the resonant peaks with the frequency of the laser field.

Acknowledgment

One of the authors PS is grateful to University of Delhi for providing the funds under the "Scheme to Strengthen Research and Development."

References

1 Rink S, Chemla D S & Miller D A B, *Adv Phys,* 38 (1989) 89.
2 Davies J H, *The physics of low dimensional semiconductors,* (Cambridge University Press), 1998.
3 Rogalski A, *J Appl Phys*, 93 (2003) 4355.
4 Prasad V & Silotia P, *Phys Lett A*, 375 (2011) 3910.
5 Anchala, Purohit S P & Mathur K C, *J Appl Phys*, 110 (2011) 114320.
6 Narayanan A, Peter A J & Yoo C K, *Physics B*, 409 (2013) 433.
7 Dingle R, Wiegmann W & Henry C H, *Phys Rev Lett*, (1974) 827.
8 Reed M, *Nanostructured Systems,* (Academic Press, San Diego), 1992.
9 Ferreira R & Bastard G, *Rep Prog Phys*, 60 (1996) 345.
10 Prasad V & Dahiya B, *Physica Status Solidi B,* 248 (2011) 1727.
11 Choi K K, *The physics of quantum well infrared photodetectors,* (World Scientific, Singapore), 1999.
12 Chang L L, Esaki L & Tsu R, *Appl Phys Lett*, 24 (1974) 593.
13 Peralta X G, Allen S J, Wanke M C, Harff N E, Simmons J A, Lilly M P, Reno J L, Burke P J & Eisenstein J P, *Appl Phys Lett*, 81 (2002) 1627.
14 Albo A, Fekete D, Bahir G, *J Appl Phys*, 112 (2012) 084502.
15 Li Y, Qian F, Xiang J & Lieber C M, *Mater Today*, 9 (2006) 18.
16 Miller D A B, Chemla D S, Damen T C, Gosaard A C, Wiegmann W, Wood T H & Barrus C A , *Appl Phys Lett*, 45 (1984) 13.
17 Miller D A B, *Int J High Speed Electron*, 1 (1990) 19.
18 May-Arrioja D A, Bickel N, Alejo-Molina A, Torres-Cisneros M, Sanchez-Mondragon J J & LiKam W P, *Microelectron J*, 40 (2009) 574.
19 Kan Y, Nagai H, Yamanishi M & Suemune I, *IEEE J Quant Electron*, 23(1987) 2167
20 Chuang S L & Ahn D, *J Appl Phys*, 65 (1989) 2822.
21 Shi J J & Pan S H, *Superlattice Microstruct*, 17 (1995) 91.
22 Shim H W, Choi R J, Jeong S M, Vinh L V, Hong C H, Suh E K, Kim Y W & Hwang Y G, *Appl Phys Lett*, 81 (2002) 3552.
23 Shim H W, Suh E K, Hong C H, Kim Y W & Lee H J, *Phys Status Solidi A*, 200 (2003) 62.
24 Choi R J, Han Y B, Shim H W, Han M S, Suh E K & Lee H J, *Appl Phys Lett*, 82 (2003) 2764.
25 Chen Bin, Guo Kang-Xian, R Z Wang & Zhang Z H, *Superlattice Microstruct*, 45 (2009) 125.
26 Chen B, Guo K X, Wang R Z, Zhang Z H & Liu Z L, *Solid State Commun*, 149 (2009) 310.
27 Dahiya B, Prasad V & Yamashita K, *J Luminescence*, 136 (2013) 240.
28 Chen B, Guo K X, Wang R Z, Zheng Y B & Li B, *Eur Phys J B*, 66 (2008) 227.
29 Karabulut I, Safak H & Tomak M, *Solid State Commun*, 135 (2005) 735.
30 Karabulut I & Safak H, *Physica B*, 368 (2005) 82.
31 Zhang L & Xie H J, *Phys Rev B*, 68 (2003) 235315.
32 Ozturk E & Sokmen I, *Superlattice Microstruct*, 48 (2010) 312.
33 Hassanabadi H, Liu G & Lu L, *Solid State Commun*, 152 (2012) 1761.
34 Ozturk E & Sokmen I, *Superlattice Microstruct,* 50 (2011) 4350.
35 Ramirez H Y & Camacho A S, Lew Yan Voon L C, *Nanotechnol*, 17(2006) 1286.
36 Silotia P, Batra K & Prasad V, *Opt Eng*, 53 (2014) 027105.
37 Ahn D & Chuang S L, *IEEE J Quant Electron*, 23 (1987) 2196.
38 Unlu S, Karabulut I & Safak H, *Phys E*, 33 (2006) 319.
39 Silotia P, Joshi H & Prasad V, *Phys Lett A*, 378 (2014) 3561.